

Heavier Alkali Metal Complexes of a Silicon- and Phosphine-Borane-Stabilized Carbanion

Keith Izod,* Corinne Wills, William Clegg, and Ross W. Harrington

Department of Chemistry, School of Natural Sciences, Bedson Building, University of Newcastle, Newcastle upon Tyne, NE1 7RU, U.K.

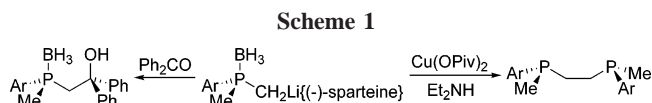
Received July 5, 2006

Treatment of the phosphine-borane adduct $(\text{Me}_3\text{Si})_2\{\text{Me}_2\text{P}(\text{BH}_3)\}\text{CH}$ (**5**) with either MeNa or MeK in diethyl ether yields the corresponding alkali metal salts $[(\text{Me}_3\text{Si})_2\{\text{Me}_2\text{P}(\text{BH}_3)\}\text{C}]\text{ML}_\infty$ [$\text{ML} = \text{Na}(\text{THF})_2 \cdot 1/2\text{PhMe}$ (**6a**); K (**7**)] after recrystallization. Metathesis reactions between in situ prepared $[(\text{Me}_3\text{Si})_2\{\text{Me}_2\text{P}(\text{BH}_3)\}\text{C}]\text{Li}$ and either rubidium or cesium 2-ethylhexoxide give the compounds $[(\text{Me}_3\text{Si})_2\{\text{Me}_2\text{P}(\text{BH}_3)\}\text{C}]\text{ML}_n$ [$\text{ML} = \text{Rb}$, $n = \infty$ (**10**); Cs(pmdeta), $n = 2$ (**11**)] after recrystallization. Compounds **6a**, **7**, **10**, and **11** are the first heavier alkali metal complexes of a phosphine-borane-stabilized carbanion to be isolated in the solid state. Compounds **5**, **6a**, **7**, **10**, and **11** have been characterized by elemental analyses, multielement (^1H , $^{13}\text{C}\{^1\text{H}\}$, $^{11}\text{B}\{^1\text{H}\}$, and $^{31}\text{P}\{^1\text{H}\}$) NMR spectroscopy, and X-ray crystallography. In the solid state compounds **6a**, **7**, **10**, and **11** adopt dimeric or polymeric structures in which the alkali metal cations are associated with both the carbanion centers and the borane hydrogen atoms.

Introduction

Tertiary phosphine-borane adducts $\text{R}_3\text{P}-\text{BH}_3$ are characterized by several important features:¹ (i) the P–B bond is particularly stable, so the phosphorus centers in such compounds are effectively protected toward oxidation; (ii) typically, the borane function in these adducts is relatively inert; (iii) adduct formation is usually reversible and, in general, both formation and cleavage of *P*-chiral phosphine-boranes occurs with retention of configuration at phosphorus; and (iv) CH protons α to the phosphorus atom are activated toward deprotonation, affording highly stabilized carbanions.¹ These properties have been widely exploited, and phosphine-borane-stabilized carbanions have become key intermediates in the synthesis of both achiral and chiral phosphines, many of which have applications as ligands for transition metal-based catalysts.² For example, Evans and co-workers have shown that the phosphine-borane-stabilized carbanion complexes $[\text{ArMeP}(\text{BH}_3)\text{CH}_2]\text{Li}\{(-)\text{-sparteine}\}$ may be readily derivatized to give a wide variety of homochiral mono- or polyphosphines, such as the chiral diphosphine DIPAMP, stereoselectively (Scheme 1).^{2b}

Phosphine-borane-stabilized carbanions are typically prepared via the α -deprotonation of a phosphine-borane adduct by a strong base such as LDA or BuLi; the lithium complexes so formed are normally generated and used in situ. Despite the ubiquity of these intermediates, little is known about their structures in either the solid state or solution, even though such information is of vital importance in understanding the reactivity and selectivity of these species. To date only four α -lithiated



phosphine-boranes have been structurally characterized, each of which adopts a different structural motif in the solid state; there have been no reports of analogous compounds containing the heavier alkali metals. The first structurally characterized α -lithiated phosphine-borane was reported by Schmidbaur and co-workers in 1979: $[\text{CH}\{\text{Me}_2\text{P}(\text{BH}_3)\}_2][\text{Li}(\text{tmeda})_2]$ (**1**) crystallizes as a separated ion pair with no short contacts between the cation and anion (Chart 1) [tmeda = *N,N,N',N'*-tetramethylethylenediamine].³ Subsequently, we reported the synthesis and structural characterization of the unusual dicarbanion complex $[(\text{Me}_3\text{Si})\{n\text{-Pr}_2\text{P}(\text{BH}_3)\}\text{CCH}_2]\text{Li}(\text{pmdeta})_2$ (**2**), which exhibits contacts between the lithium ions and the borane hydrogen atoms, but not between lithium and the carbanion centers [pmdeta = *N,N,N',N',N''*-pentamethyldiethylenetriamine].⁴ Shortly after our report, Kobayashi and co-workers reported the structure of the α -lithiated phospholane-borane adduct **3**, which exhibits a Li–C contact, but no Li–BH₃ contacts.⁵ Most recently, we reported the synthesis of the ate complex $(\text{THF})_3\text{Li}\{(\text{Me}_3\text{Si})_2\text{CPMe}_2(\text{BH}_3)_2\}_2\text{Li}$ (**4**), which exhibits both Li–C and Li \cdots H₃B contacts in the solid state.⁶

We have previously demonstrated that the selectivity of reactions involving phosphine-borane-stabilized carbanions is markedly affected by their structures. For example, whereas reactions between the α -metalated phosphine-boranes $[\text{ArMePCH}_2]\text{Li}\{(-)\text{-sparteine}\}$ (Ar = e.g., Ph, *o*-tolyl, *o*-anisyl) and electrophiles typically proceed with high stereoselectivity (Scheme

* Corresponding author. E-mail: e-mail: k.j.izod@ncl.ac.uk.

(1) For reviews of phosphine-borane chemistry see: (a) Schmidbaur, H. *J. Organomet. Chem.* **1980**, *200*, 287. (b) Carboni, B.; Monnier, L. *Tetrahedron* **1999**, *55*, 1197. (c) Brunel, J. M.; Faure, B.; Maffei, M. *Coord. Chem. Rev.* **1998**, *178–180*, 665. (d) Paine, R. T.; Nöth, H. *Chem. Rev.* **1995**, *95*, 343. (e) Gaumont, A. C.; Carboni, B. In *Science of Synthesis*, Vol. 6; Kaufmann, D., Matteson, D. S., Eds.; Thieme: Stuttgart, 2004; pp 485–512.

(2) (a) Ohff, M.; Holz, J.; Quirmbach, M.; Börner, A. *Synthesis* **1998**, 1391. (b) Muci, A. R.; Campos, K. R.; Evans, D. A. *J. Am. Chem. Soc.* **1995**, *117*, 9075. (c) Imamoto, T. *Pure Appl. Chem.* **1993**, *65*, 655.

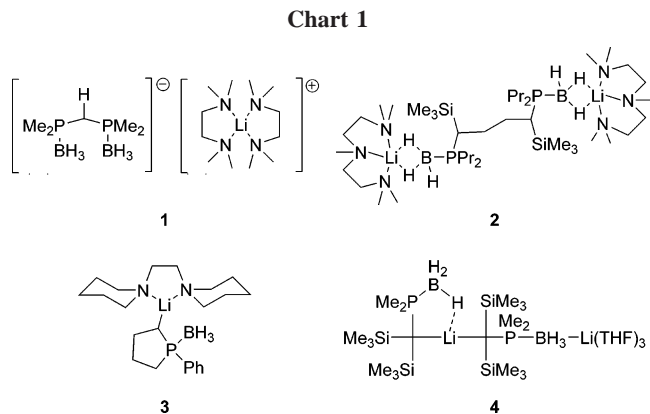
(3) Schmidbaur, H.; Weiss, E.; Zimmer-Gasser, B. *Angew. Chem., Int. Ed. Engl.* **1979**, *18*, 782.

(4) Izod, K.; McFarlane, W.; Tyson, B. V.; Clegg, W.; Harrington, R. W. *Chem. Commun.* **2004**, 570.

(5) Sun, X.-M.; Manabe, K.; Lam, W. W.-L.; Shiraishi, N.; Kobayashi, J.; Shiro, M.; Utsumi, H.; Kobayashi, S. *Chem. Eur. J.* **2005**, *11*, 361.

(6) Izod, K.; Wills, C.; Clegg, W.; Harrington, R. W. *Organometallics* **2006**, *25*, 38.

Chart 1



1), we find that the absence of a significant Li–C contact in $[[(\text{Me}_3\text{Si})\{n\text{-Pr}_2\text{P}(\text{BH}_3)\}\text{CCH}_2]\text{Li}\{(-)\text{-sparteine}\}]_2$ (**2a**) results in a complete lack of stereoselectivity in its reactions with electrophiles.⁴

To achieve a better understanding of the relationship between structure and reactivity in phosphine-borane-stabilized carbanions, we have begun a detailed study of these compounds. We now present our initial results from this study, which address the effect of cation size and polarizability on the solid and solution state structures of complexes of the heavier alkali metals with the sterically hindered phosphine-borane-stabilized carbanion $(\text{Me}_3\text{Si})_2\{\text{Me}_2\text{P}(\text{BH}_3)\}\text{C}^-$. These compounds constitute the first heavier alkali metal complexes of a phosphine-borane-stabilized carbanion to be structurally characterized.

Results and Discussion

Syntheses and Solid State Structures. Treatment of the readily accessible primary chlorophosphine $(\text{Me}_3\text{Si})_2\text{CHPCl}_2$ with 2 equiv of MeMgBr followed by 1 equiv of $\text{BH}_3\cdot\text{SMe}_2$ conveniently gives the air-stable adduct $(\text{Me}_3\text{Si})_2\{\text{Me}_2\text{P}(\text{BH}_3)\}\text{-CH}$ (**5**) in excellent yield. Compound **5** is obtained essentially pure by this method, but may be recrystallized as colorless blocks from cold methylcyclohexane containing a few drops of THF. [The syntheses of **5** and its lithium derivative **4** have been described in detail in a previous communication.⁶] To gain insight into the effect of metalation on the bond lengths and angles within phosphine-borane adducts, we have carried out a single-crystal X-ray diffraction study of **5**. The molecular structure of **5** is shown in Figure 1, along with details of selected bond lengths and angles. The structure is unsurprising; the C(1)–Si(1) and C(1)–Si(2) distances are 1.8831(13) and 1.9118(13) Å, respectively, while the C(1)–P and B–P distances are 1.8508(13) and 1.8957(17) Å, respectively. These are typical of bond lengths in other crystallographically characterized phosphine-borane adducts.⁷ The angles within the CSi_2P framework lie in a small range close to 114° (sum of angles within the CSi_2P skeleton = 341.45°).

Reactions between **5** and 1 equiv of either MeNa or MeK in cold diethyl ether give the compounds $[(\text{Me}_3\text{Si})_2\{\text{Me}_2\text{P}(\text{BH}_3)\}\text{C}]\text{M}$ [M = Na (**6**), K (**7**)] as viscous yellow to orange

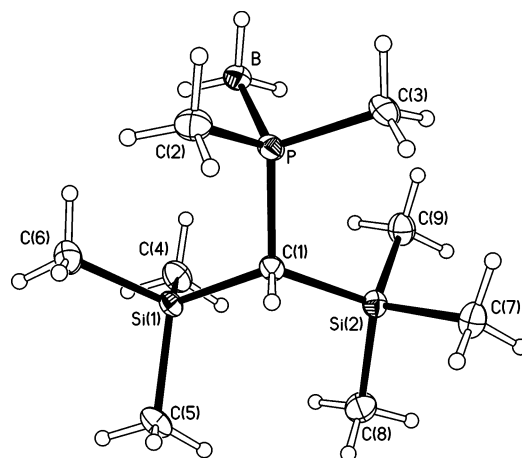
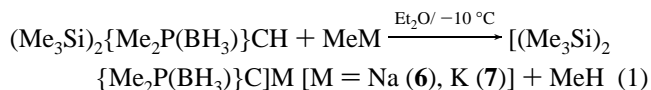


Figure 1. Molecular structure of **5** with 40% probability ellipsoids. Selected bond lengths (Å) and angles (deg): P–B 1.8957(17), P–C(1) 1.8508(13), Si(1)–C(1) 1.8831(13), Si(2)–C(1) 1.9118(13), mean Si–C(Me) 1.8631, Si(1)–C(1)–Si(2) 113.82(7), Si(1)–C(1)–P 113.44(6), Si(2)–C(1)–P 114.19(7).

oils after a simple workup (eq 1). Recrystallization of **6** from cold toluene containing a few drops of THF gives the adduct $[(\text{Me}_3\text{Si})_2\{\text{Me}_2\text{P}(\text{BH}_3)\}\text{C}]\text{Na}(\text{THF})_2\cdot 1/2\text{PhMe}]_\infty$ (**6a**) as colorless needles. The corresponding potassium salt $[(\text{Me}_3\text{Si})_2\{\text{Me}_2\text{P}(\text{BH}_3)\}\text{C}]\text{K}_\infty$ (**7**) may be obtained solvent-free as colorless blocks by recrystallization from hot benzene; we were unable to crystallize **6** in the absence of coordinating solvent. The room-temperature ^1H , $^{13}\text{C}\{^1\text{H}\}$, $^{11}\text{B}\{^1\text{H}\}$, and $^{31}\text{P}\{^1\text{H}\}$ NMR spectra of **6a** and **7** are as expected (see below); however, both the toluene of crystallization and the coordinated THF in **6a** are rapidly lost under vacuum, and so the elemental analyses and NMR spectra of samples exposed to vacuum for a few minutes show no signs of these solvents.



The solid state structures of **6a** and **7** were determined by X-ray crystallography; the structures of **6a** and **7** are shown in Figures 2 and 3, respectively, along with details of selected bond lengths and angles. Compound **6a** crystallizes as a one-dimensional zigzag polymer. Each sodium ion is coordinated by the carbanion center of one ligand and by an $\eta^2\text{-BH}_3$ group of an adjacent ligand; thus the phosphine-borane-stabilized carbanions act as bridging ligands between adjacent sodium ions in the chain, which is generated by screw-axis symmetry. The coordination sphere of each sodium ion is completed by the oxygen atoms of two molecules of THF, giving a pseudo-four-coordinate sodium ion with a distorted tetrahedral geometry.

The carbanion in **6a** is exactly isoelectronic with the tris(trimethylsilyl)methyl carbanion, and so it is instructive to compare the structure of **6a** with that of the corresponding tris(trimethylsilyl)methylsodium complex, $[(\text{Me}_3\text{Si})_3\text{C}]_2\text{Na}[\text{Na}(\text{tmeda})_2(\text{OEt}_2)]$ (**8**).⁸ Most strikingly, while compound **6a** crystallizes as a one-dimensional polymer, compound **8** crystallizes as a separated ion pair dialkylsodiate complex. This would appear to be a consequence of the ability of the BH_3 hydrogen atoms to coordinate to metal centers. In contrast, the lithium complex $(\text{THF})_3\text{Li}\{(\text{Me}_3\text{Si})_2\text{CPMe}_2(\text{BH}_3)\}_2\text{Li}$ (**4**) does crystallize as a dialkylmetalate complex,⁶ closely related to the tris-

(7) For examples see: (a) Takahashi, Y.; Yamamoto, Y.; Katagiri, K.; Danjo, H.; Yamaguchi, K.; Imamoto, T. *J. Org. Chem.* **2005**, *70*, 9009. (b) Dilsky, S.; Schenk, W. A. Z. *Naturforsch. B* **2004**, *59*, 1093. (c) Merle, N.; Kociok-Kohn, G.; Mahon, M. F.; Frost, C. G.; Ruggiero, G. D.; Weller, A. S.; Willis, M. C. *Dalton Trans.* **2004**, 3883. (d) Wyatt, P.; Eley, H.; Charmant, J.; Daniel, B. J.; Kantacha, A. *Eur. J. Org. Chem.* **2003**, 4216. (e) Cotton, F. A.; Murillo, C. A.; Wang, X. *J. Am. Chem. Soc.* **1998**, *120*, 9594. (f) Graf, C.-D.; Malan, C.; Harms, K.; Knochel, P. *J. Org. Chem.* **1999**, *64*, 5581. (g) Huffman, J. C.; Skupinski, W. A.; Caulton, K. G. *Cryst. Struct. Commun.* **1982**, *11*, 1435.

(8) Al-Juaid, S. S.; Eaborn, C.; Hitchcock, P. B.; Izod, K.; Mallien, M.; Smith, J. D. *Angew. Chem., Int. Ed. Engl.* **1994**, *33*, 1268.

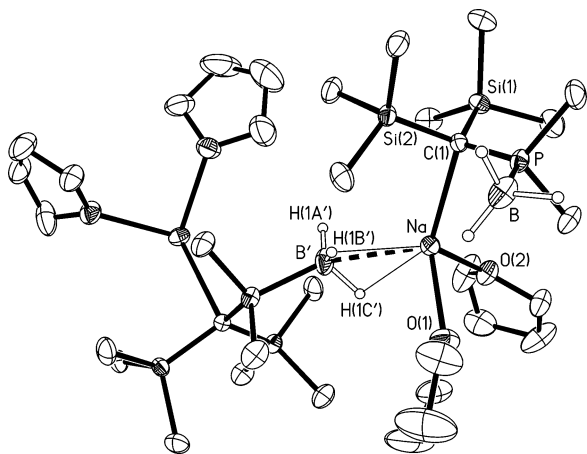


Figure 2. Structure of **6a** with 40% probability ellipsoids and selected atom labels. Solvent of crystallization, H atoms bonded to carbon, and minor disorder components omitted for clarity. Selected bond lengths (Å) and angles (deg): Na–C(1) 2.640(3), Na–O(1) 2.361(2), Na–O(2) 2.357(2), Na–H(1B') 2.26(3), Na–H(1C') 2.46(3), Na···B' 2.766(3), P–C(1) 1.752(2), Si(1)–C(1) 1.853(3), Si(2)–C(2) 1.858(2), P–B 1.941(4), O(1)–Na–O(2) 90.39(8), O(1)–Na–C(1) 123.13(9), O(1)–Na···B' 100.32(11), O(2)–Na–C(1) 116.19(8), O(2)–Na···B' 99.04(10), C(1)–Na···B' 121.36(10). Atoms generated by screw-axis symmetry are primed.

(trimethylsilyl)methyl analogues $\{[(\text{Me}_3\text{Si})_3\text{C}]_2\text{Li}][\text{Li}(\text{L})_n][\text{Li}(\text{L})_n] = \text{Li}(\text{THF})_4, \text{Li}(\text{tmeda})_2, (\text{pmdeta})\text{LiClLi}(\text{pmdeta})\}$.⁹ The Na–C(1) distance of 2.640(3) Å in **6a** is somewhat longer than the corresponding distance of 2.479(6) Å in **8**.⁸ Indeed, the Na–C distance in **6a** is rather long for this type of contact, which typically falls in the range 2.48–2.55 Å;¹⁰ for example, the Na–C distance in $\{[(\text{Me}_3\text{Si})_2\text{CH}]\text{Na}\}_\infty$ is 2.555(10) Å.¹¹ The Na–H distances of 2.26(3) and 2.46(3) Å and the Na···B distance of 2.766(3) Å are similar to the Na–H and Na···B distances in several complexes of sodium tetrahydroborate; for example, the Na–H distances in $[(\text{pmdeta})\text{Na}(\mu\text{-BH}_4)]_2$ range from 2.49(3) to 2.58(3) Å, and the Na···B distances in this compound are 2.727(4) and 2.867(4) Å.¹² The CSi_2P skeleton in **6a** is only slightly less pyramidal than that in the free phosphine-borane **5** (sum of angles in the CSi_2P skeleton of **6a** = 346.29°). The Si(1)–C(1), Si(2)–C(1), and P–C(1) distances of 1.853(3), 1.858(2), and 1.752(2) Å, respectively, are substantially shorter than the corresponding distances in **5**, consistent with significant delocalization of charge away from the carbanion center via negative hyperconjugation and/or polarization effects.

Compound **7** is also polymeric in the solid state; however, **7** crystallizes as a rather complex two-dimensional sheet in which there are two distinct potassium environments and two distinct ligand environments. K(1) is coordinated by both the carbanion center and an $\eta^2\text{-BH}_3$ group of ligand 1, forming a pseudo-four-membered chelate ring, and by the BH_3 groups of ligand 2 and its inversion-symmetry equivalent. The BH_3 groups of

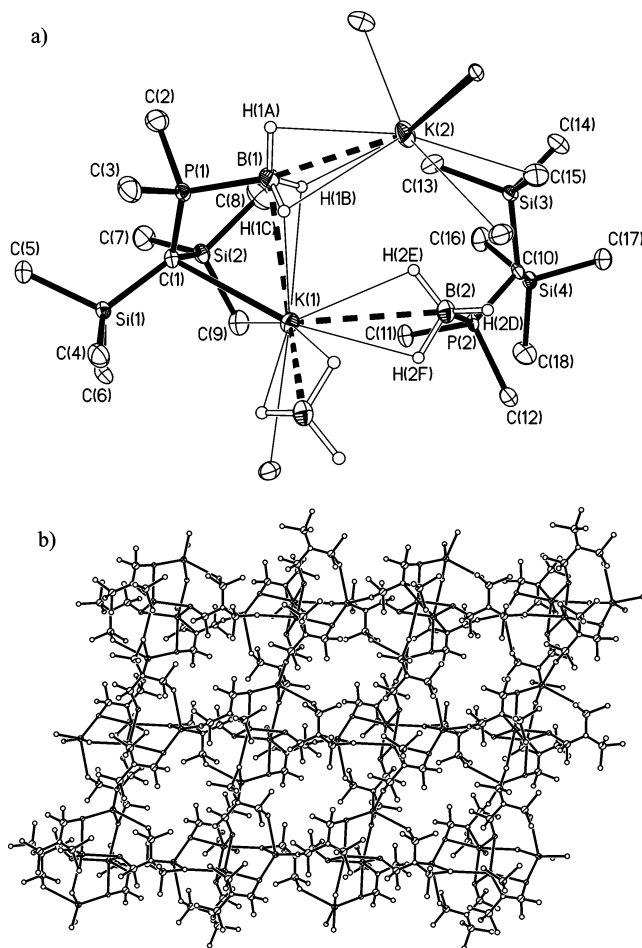


Figure 3. (a) Structure of the asymmetric unit of **7** (two K^+ ions and two ligands), together with additional symmetry-related atoms (unlabeled) to complete the coordination of K(1) and K(2), with 40% probability ellipsoids and with H atoms bonded to carbon omitted for clarity. (b) Sheet structure of **7**, with all H atoms omitted. Details of selected bond lengths (Å) and angles (deg) for **7** (values in square brackets refer to the isostructural compound **10**): M(1)–C(1) 3.018(5) [3.154(3)], M(1)–H(1B) 2.87(5) [2.97(3)], M(1)–H(1C) 2.74(5) [2.76(3)], M(1)–H(2E) 2.85(6) [3.03(3)], M(1)–H(2F) 2.82(5) [2.95(3)], M(1)–H(2Db) 2.76(5) [2.90(3)], M(1)–H(2Fb) 2.86(5) [2.91(3)], M(1)···B(1) 3.108(7) [3.233(4)], M(1)···B(2) 3.340(7) [3.477(4)], M(1)···B(2b) 3.266(7) [3.388(4)], M(1)···C(9) 3.507(6) [3.550(4)], M(1)···C(17a) 3.393(5) [3.406(3)], M(2)–C(10d) 3.001(5) [3.175(3)], M(2)–H(1A) 2.74(5) [2.89(4)], M(2)–H(1B) 2.71(5) [2.82(3)], M(2)–H(1C) 2.92(5) [3.13(3)], M(2)···B(1) 2.946(6) [3.106(4)], M(2)···C(4c) 3.234(6) [3.405(3)], M(2)···C(15) 3.456(6) [3.540(4)], M(2)···C(17d) 3.421(6) [3.588(3)], P(1)–C(1) 1.735(5) [1.746(3)], Si(1)–C(1) 1.835(5) [1.842(3)], Si(2)–C(1) 1.843(5) [1.843(3)], P(1)–B(1) 1.933(6) [1.942(4)], P(2)–C(10) 1.735(5) [1.746(3)], Si(3)–C(10) 1.844(5) [1.844(3)], Si(4)–C(10) 1.842(5) [1.842(3)], P(2)–B(2) 1.932(7) [1.943(4)], P(1)–C(1)–Si(1) 120.4(3) [120.94(18)], P(1)–C(1)–Si(2) 116.6(3) [116.91(16)], Si(1)–C(1)–Si(2) 116.5(3) [116.86(17)], P(2)–C(10)–Si(3) 115.4(3) [115.80(16)], P(2)–C(10)–Si(4) 118.3(3) [118.45(17)], Si(3)–C(10)–Si(4) 115.0(3) [116.00(15)].

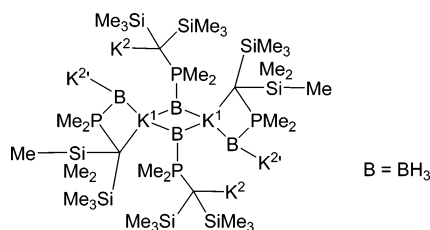
ligand 2 form $\mu_2\text{-}\eta^2\text{-}\eta^2$ -bridges between K(1) and the inversion-related K(1b) to give a $\text{K}_2(\text{BH}_3)_2$ pseudo-four-membered ring. The BH_3 group of ligand 1 also bridges K(1) and K(2) in a $\mu_2\text{-}\eta^2\text{-}\eta^3$ -fashion; K(2) is further coordinated by the carbanion center of a symmetry-related ligand 2. Thus ligand 1 both chelates K(1) and bridges between K(1) and K(2) via a $\mu_2\text{-}\eta^2\text{-}\eta^3\text{-BH}_3$ group, whereas ligand 2 acts as both a $\mu_2\text{-}\eta^2\text{-}\eta^2\text{-BH}_3$ bridge between K(1) and K(1b) and as a bridge between K(1/

(9) (a) Eaborn, C.; Hitchcock, P. B.; Smith, J. D.; Sullivan, A. C. *J. Chem. Soc., Chem. Commun.* **1983**, 827. (b) Avent, A. G.; Eaborn, C.; Hitchcock, P. B.; Lawless, G. A.; Lickiss, P. D.; Mallein, M.; Smith, J. D.; Webb, A.; Wrackmeyer, B. *J. Chem. Soc., Dalton Trans.* **1993**, 3259. (c) Buttrus, N. H.; Eaborn, C.; Hitchcock, P. B.; Smith, J. D.; Stamper, J. G.; Sullivan, A. C. *J. Chem. Soc., Chem. Commun.* **1986**, 969.

(10) (a) Schade, C.; Schleyer, P. von R. *Adv. Organomet. Chem.* **1987**, 27, 169. (b) Smith, J. D. *Adv. Organomet. Chem.* **1999**, 43, 267.

(11) Hitchcock, P. B.; Lappert, M. F.; Leung, W.-P.; Diansheng, L.; Shun, T. *J. Chem. Soc., Chem. Commun.* **1993**, 1386.

(12) Giese, H.-H.; Haberer, T.; Nöth, H.; Ponikvar, W.; Thomas, S.; Warchold, M. *Inorg. Chem.* **1999**, 38, 4188.

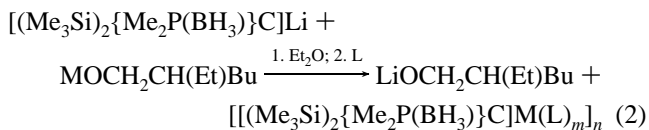
Chart 2. Principal Metal–Ligand Contacts in **7**

1b) and a symmetry equivalent of K(2) via its carbanion center and its BH₃ group (Chart 2). The coordination spheres of K(1) and K(2) are completed by either two or three short agostic-type K \cdots Me–Si contacts, respectively [K(1) \cdots C(9) 3.507(6), K(1) \cdots C(17a) 3.393(5), K(2) \cdots C(17d) 3.421(6), K(2) \cdots C(15) 3.457(6), K(2) \cdots C(4c) 3.2346 Å]; one methyl group [C(17)] bridges the two different potassium ions via this type of interaction. The K(1)–C(1) and K(2)–C(10d) distances of 3.018(5) and 3.001(5) Å, respectively, are typical for this type of contact (K–C σ -bonds typically lie in the range 2.91–3.10 Å).¹⁰

Once again, comparison of the structure of **7** with the isoelectronic analogue $\{[(\text{Me}_3\text{Si})_3\text{C}]\text{K}\}_\infty$ (**9**) is informative.¹³ While both compounds crystallize solvent-free, **9** crystallizes as a linear polymer of alternating potassium cations and planar carbanions, with additional, short, agostic-type K \cdots Me–Si contacts to three Si–Me groups from each adjacent ligand, whereas **7** crystallizes as a sheet polymer containing K–C, K–H₃B, and K \cdots Me–Si contacts. The K–C(1) distances in **9** of 3.090(11) and 3.104(1) Å are similar to those in **7**. The K \cdots Me contacts in **7** are somewhat longer than the corresponding distances in **9**, which span the range 3.187(13)–3.311(11) Å, reflecting the increased formal coordination number of the potassium ions in **7** due to coordination of the BH₃ groups. Both potassium ions in **7** exhibit strong contacts with the BH₃ hydrogen atoms. The K–H distances in **7** range from 2.71(5) to 2.92(4) Å, and the K \cdots B distances range from 3.108(7) to 3.340(7) Å; these compare with K–H distances of 2.56(2), 2.67(1), and 3.06(2) Å and a K \cdots B distance of 3.292(2) Å in $\{[\text{K}(\text{H}_2\text{B}-t\text{-Bu}_2)(\text{pmdeta})]_2\}$.¹⁴ The carbanion centers in **7** are somewhat closer to planar than those in **6a** and **4** (sum of angles in the CSi₂P skeleton at C(1) = 353.5°; C(10) = 348.7°).

Since MeRb and MeCs are rather difficult materials to isolate and handle,¹⁵ we chose a metathetical route for the synthesis of the rubidium and cesium derivatives of $(\text{Me}_3\text{Si})_2\{\text{Me}_2\text{P}(\text{BH}_3)\}\text{C}^-$. The reaction between in situ-prepared $[(\text{Me}_3\text{Si})_2\{\text{Me}_2\text{P}(\text{BH}_3)\}\text{C}]\text{Li}$ and 1 equiv of rubidium 2-ethylhexoxide in diethyl ether, followed by recrystallization from hot methylcyclohexane, cleanly yields the salt $[(\text{Me}_3\text{Si})_2\{\text{Me}_2\text{P}(\text{BH}_3)\}\text{C}]\text{Rb}$ (**10**) as colorless plates suitable for X-ray crystallography. A similar reaction between $[(\text{Me}_3\text{Si})_2\{\text{Me}_2\text{P}(\text{BH}_3)\}\text{C}]\text{Li}$ and 1 equiv of cesium 2-ethylhexoxide in diethyl ether yields the corresponding cesium salt (eq 2). However, somewhat unexpectedly, the cesium salt is highly soluble, even in light petroleum, and so it is necessary to extract the lithium 2-ethylhexoxide side-product from this metathesis reaction into hexamethyldisiloxane. This extremely poor solvent dissolves the lithium alkoxide, leaving essentially pure $[(\text{Me}_3\text{Si})_2\{\text{Me}_2\text{P}(\text{BH}_3)\}\text{C}]\text{Cs}$ as a colorless oil. We were unable to crystallize this oil in the absence of co-ligands, but obtained X-ray-quality crystals of the adduct $[(\text{Me}_3\text{Si})_2\{\text{Me}_2\text{P}(\text{BH}_3)\}\text{C}]\text{Cs}(\text{pmdeta})_2$ (**11**) in good yield from hot

methylcyclohexane containing 1 equiv of pmde_ta. Once again, the NMR spectra of **10** and **11** are consistent with these formulations (see below).



[M = Rb, $m = 0$, $n = \infty$ (**10**); M = Cs, L = pmde_ta, $m = 1$, $n = 2$ (**11**)]

Compounds **10** and **11** are rare examples of σ -bonded organometallic derivatives of the heavier alkali metals Rb and Cs; indeed, only a handful of such compounds have been crystallographically characterized.^{10,16} Compound **10** crystallizes as a two-dimensional sheet polymer that is both isomorphous and isomorphous with **7**; details of selected bond lengths and angles are given in the caption to Figure 3. The Rb(1)–C(1) and Rb(2)–C(10d) distances of 3.154(3) and 3.175(3) Å, respectively, are rather short compared to the range of previously reported Rb–C σ -bonding distances (3.29–3.51 Å).¹⁰ For comparison, the Rb–C distances in the isoelectronic compound $\{[(\text{Me}_3\text{Si})_3\text{C}]\text{Rb}\}_\infty$ are 3.291(7) and 3.287(7) Å^{16a} and the Rb–C distances in $\{[(\text{Me}_3\text{Si})_2\text{CH}]\text{Rb}(\text{pmdeta})\}_2$ are 3.361(9) and 3.485(8) Å.¹¹ The Rb–H distances range from 2.76(3) to 3.13–(3) Å and the Rb \cdots B distances range from 3.106(4) to 3.477–(4) Å; these compare with Rb–H distances ranging from 2.49 to 3.17 Å and Rb \cdots B distances ranging from 3.084 to 3.419 Å in Rb₂[B₁₀H₁₀] and Rb₂[B₉H₉].¹⁷

Compound **11** adopts a dimeric structure in the solid state, the two halves of which are related by an inversion center halfway along the Cs \cdots Cs vector; the molecular structure of **11** is shown in Figure 4, along with details of selected bond lengths and angles. Each cesium ion is coordinated by the carbanion center and one hydrogen atom of the BH₃ group of one ligand. This BH₃ group bridges in an η^3 -fashion to the second cesium ion in the dimer; thus each cesium ion is coordinated by one η^1 - and one η^3 -BH₃ group. The coordination sphere of each cesium ion is completed by the three nitrogen atoms of a molecule of pmde_ta and agostic-type interactions with one methyl group from the PMe₂ substituent, one methyl group from one of the Me₃Si substituents, and four methyl groups from the pmde_ta ligand [the Cs \cdots C(Me) distances span the range 3.629(6)–3.881(5) Å]. The Cs–C(1) distance of 3.549(4) Å is rather long in comparison to other Cs–C σ -bonds;^{10,16} for example, the Cs–C distances in the closely related compounds $\{(\text{Me}_3\text{Si})_3\text{C}\}\text{Cs}(\text{C}_6\text{H}_6)_3\cdot\text{C}_6\text{H}_6$ ^{16a} and $\{[(\text{Me}_3\text{Si})_2\text{CH}]\text{Cs}(\text{tmeda})\}_\infty$ ^{16d} are 3.332(5) and 3.425(2) Å, respectively. The Cs–H distances range from 3.09(5) to 3.45(5) Å and the Cs \cdots B(1) and Cs \cdots B(1A) distances are 3.990(7) and 3.380(6) Å, respectively. These compare with Cs–H distances ranging from 3.19 to 3.38 Å and Cs \cdots B distances ranging from

(13) Eaborn, C.; Hitchcock, P. B.; Izod, K.; Jaggar, A. J.; Smith, J. D. *Organometallics* **1994**, *13*, 753.

(14) Knizek, J.; Nöth, H. *J. Organomet. Chem.* **2000**, *614–615*, 168.

(15) Weiss, E. *Angew. Chem., Int. Ed. Engl.* **1993**, *32*, 1501.

(16) (a) Eaborn, C.; Hitchcock, P. B.; Izod, K.; Smith, J. D. *Angew. Chem., Int. Ed. Engl.* **1995**, *34*, 687. (b) Eaborn, C.; Hitchcock, P. B.; Smith, J. D.; Zhang, S.; Clegg, W.; Izod, K.; O'Shaughnessy, P. *Organometallics* **2000**, *19*, 1190. (c) Eaborn, C.; Clegg, W.; Hitchcock, P. B.; Hopman, M.; Izod, K.; O'Shaughnessy, P. N.; Smith, J. D. *Organometallics* **1997**, *16*, 4728. (d) Boesveld, W. M.; Hitchcock, P. B.; Lappert, M. F.; Liu, D.-S.; Tian, S. *Organometallics* **2000**, *19*, 4030. (e) Alexander, J. S.; Allis, D. G.; Hudson, B. S.; Ruhlandt-Senge, K. *J. Am. Chem. Soc.* **2003**, *125*, 15002. (f) Hoffmann, D.; Bauer, W.; Schleyer, P. von R.; Pieper, U.; Stalke, D. *Organometallics* **1993**, *12*, 1193.

(17) (a) Hoffman, K.; Albert, B. Z. *Kristallogr.* **2005**, *220*, 142. (b) Guggenberger, L. *J. Inorg. Chem.* **1968**, *7*, 2260.

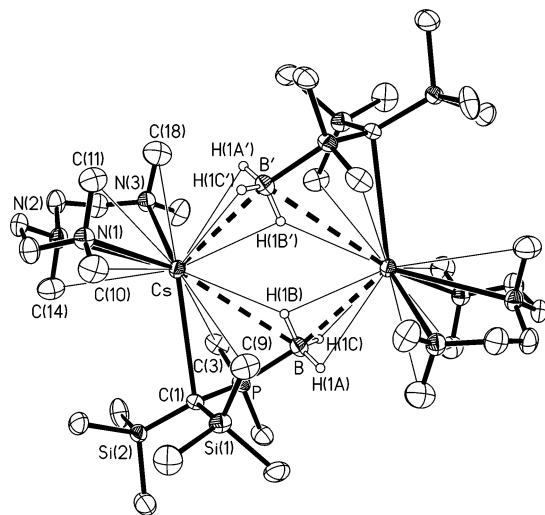


Figure 4. Molecular structure of **11** with 40% probability ellipsoids and selected atom labels, and with H atoms bonded to carbon omitted for clarity. Selected bond lengths (Å) and angles (deg): Cs–C(1) 3.549(4), Cs–N(1) 3.134(4), Cs–N(2) 3.312(4), Cs–N(3) 3.199(4), Cs–H(1B) 3.14(6), Cs–H(1A) 3.21(5), Cs–H(1B') 3.09(5), Cs–H(1C) 3.45(5), Cs···B 3.990(7), Cs(1)···B' 3.380(6), Cs···C(3) 3.881(5), Cs···C(9) 3.637(5), Cs···C(10) 3.803(6), Cs···C(11) 3.732(6), Cs···C(14) 3.628(6), Cs···C(18) 3.694(6), P–C(1) 1.743(4), Si(1)–C(1) 1.835(4), Si(2)–C(1) 1.824(4), P–B 1.929(6), C(1)–Cs···B 49.02(11), B···Cs···B' 85.04(15), N(1)–Cs–N(2) 54.84(10), N(2)–Cs–N(3) 54.58(10), P–C(1)–Si(1) 114.4(2), P–C(1)–Si(2) 119.3(2), Si(1)–C(1)–Si(2) 117.2(2).

3.579 to 3.929 Å in Cs[B₉H₁₄] and Cs₂[B₆H₆].¹⁸ The Cs–N distances are typical for this type of contact.¹⁰

A comparison of the bond lengths and angles within the neutral phosphine-borane adduct **5** and its alkali metal derivatives **4**, **6a**, **7**, **10**, and **11** reveals that metalation leads to a significant decrease in the C(1)–P distance from 1.8508(13) Å in **5** to between 1.735(5) and 1.755(5) Å, consistent with significant charge delocalization via negative hyperconjugation. There is a similar decrease in the C(1)–Si distances from 1.8831(13) and 1.9118(13) Å in **5** to between 1.824(4) and 1.858(2) Å in the metalated derivatives, suggesting that the negative charge is significantly delocalized across the whole CSi₂P skeleton, as expected. A corresponding increase in the P–B distance is observed upon metalation, from 1.8957(17) Å in **5** to between 1.926(6) and 1.944(7) Å. The nature of the alkali metal causes little variation in the angles within the CSi₂P skeleton, although the Li and Na compounds **4** and **6a** have slightly more pyramidal carbanion centers than the K, Rb, and Cs compounds **7**, **10**, and **11** [sum of angles within the CSi₂P skeleton = 344.0° and 341.7° (**4**), 346.29° (**6a**), 353.5°, 348.7° (**7**), 354.74°, 350.28° (**10**), 350.9° (**11**)]; however, the CSi₂P frameworks in **7**, **10**, and **11** are only slightly more planar than the CSi₂P skeleton in **5** [sum of angles within the CSi₂P skeleton in **5** = 341.5°]. The more pyramidal carbanion centers in **4** and **6a** are consistent with the more polarizing, charge localizing nature of the relatively small Li⁺ and Na⁺ cations.

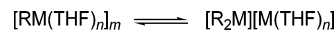
NMR Spectra and Solution State Structures. The room-temperature ¹H and ¹³C{¹H} NMR spectra of **4**, **6**, **7**, **10**, and **11** are as expected and indicate the presence of a single ligand environment on the NMR time scale. In each case the BH₃ protons give rise to very broad quartets centered between 0.40

Table 1. Selected Room-Temperature NMR Data for **4–7**, **10**, and **11** in *d*₈-Toluene

compound	¹ H{ ¹¹ B} (ppm) ^a	² J _{PH} (Hz)	¹¹ B{ ¹ H} (ppm)	³¹ P{ ¹ H} (ppm)	¹ J _{PB} (Hz)
5	1.18	13.4	–32.6	7.1	54.4
4	1.08	11.9	–28.3	–1.6	89.4
6	0.58	15.9	–28.8	–5.6	101.6
7	0.40	14.3	–27.3	–5.9	98.5
10	0.51	14.4	–26.7	–5.3	97.5
11	0.94	13.4	–25.4	–4.4	95.2

^a BH₃ protons with selective ¹¹B decoupling.

Scheme 2



and 1.08 ppm, which collapse to broad doublets on decoupling the ¹¹B nucleus (Table 1). The ¹¹B{¹H} spectra consist of broad doublets due to coupling to ³¹P; with the exception of **4**, the ¹¹B chemical shifts exhibit a gradual increase from –28.3 (**6**) to –25.4 ppm (**11**) [cf. –32.6 ppm for the neutral phosphine-borane **5**]. Metalation leads to a near doubling of the ¹¹B–³¹P coupling constant from 54.4 Hz in **5** to between 95.2 and 101.6 Hz in **6**, **7**, **10**, and **11**; with the exception of **4**, the ¹¹B–³¹P coupling constants exhibit a gradual decrease as the group is descended. The ³¹P{¹H} NMR spectra consist of broad, poorly resolved quartets at –1.6 (**4**), –5.6 (**6**), –5.9 (**7**), –5.3 (**10**), and –4.4 ppm (**11**) [cf. 7.1 ppm for **5**]. The marked differences in the ¹¹B and ³¹P spectra of **4** compared to the rest of the series suggest that compound **4** adopts a different structure in solution, consistent with the observation that, in the solid state, **4** crystallizes as a dialkylmetalate complex, whereas the other compounds are either dimeric or polymeric species containing chelating/bridging ligands.

Our preliminary studies revealed that **4** is subject to a dynamic process in *d*₈-toluene, which we attributed to an equilibrium between the ate complex observed in the solid state and either a monomeric or symmetrical oligomeric species (Scheme 2).⁶ We were interested in whether the heavier alkali metal derivatives were subject to a similar dynamic equilibrium, and so we have conducted variable-temperature ¹H, ¹¹B{¹H}, and ³¹P{¹H} NMR experiments on **6** and **10** as representative examples. However, the spectra of both **6** and **10** in *d*₈-toluene are invariant over the available temperature range, suggesting either that a single monomeric or symmetrical oligomeric species is present in each case or that any dynamic equilibrium is too fast on the NMR time scale to be observed.

Although we have established that alkali metal derivatives of phosphine-borane-stabilized carbanions frequently exhibit strong M···H–B contacts in the solid state, it is the nature of the cation–anion contacts in solution that is most likely to affect their reactivities and selectivities. In this regard, we have previously shown that the preference for Li···H–B over Li–C contacts in **2a** results in essentially no stereoselectivity in its reactions with electrophiles. To gain some insight into the nature of the cation–anion contacts in the solution state in the present series of compounds, we undertook a ¹H–¹³³Cs HOESY experiment on compound **11**. In favorable circumstances such experiments have been shown to yield excellent data concerning the proximity of protons to the Cs center;^{16f,19} the ¹³³Cs nucleus has *I* = 7/2, 100% natural abundance, but has a low quadrupole moment [*Q* = –3 × 10^{–3} Q m^{–2}], and so ¹³³Cs spectra typically exhibit only moderate quadrupolar broadening and lines are relatively sharp.

(18) (a) Greenwood, N. N.; McGinney, J. A.; Owen, J. D. *J. Chem. Soc., Dalton Trans.* **1972**, 986. (b) Kuznetsov, I. Y.; Vinitskii, D. M.; Solntsev, K. A.; Kuznetsov, N. T.; Butman, L. A. *Zh. Neorg. Khim.* **1987**, *32*, 3112.

(19) (a) Bauer, W. *Magn. Reson. Chem.* **1991**, *29*, 494. (b) Bauer, W.; Lochmann, L. *J. Am. Chem. Soc.* **1992**, *114*, 7482.

Table 2. Crystallographic Data for 5, 6a, 7, 10, and 11

	5	6a	7	10	11
formula	C ₉ H ₂₈ BPSi ₂	C ₁₇ H ₄₃ BNaO ₂ PSi ₂ · 0.5C ₇ H ₈	C ₉ H ₂₇ BKPSi ₂	C ₉ H ₂₇ BPRbSi ₂	C ₁₈ H ₅₀ BCsN ₃ PSi ₂
<i>M</i>	234.3	446.5	272.4	318.7	539.5
cryst syst	monoclinic	monoclinic	monoclinic	monoclinic	triclinic
space group	<i>P</i> 2 ₁ / <i>c</i>	<i>P</i> 2 ₁ / <i>n</i>	<i>P</i> 2 ₁ / <i>n</i>	<i>P</i> 2 ₁ / <i>n</i>	<i>P</i> $\bar{1}$
<i>a</i> /Å	8.7346(6)	9.645(2)	15.881(4)	16.216(2)	9.0555(12)
<i>b</i> /Å	14.7363(10)	13.1887(13)	13.618(4)	13.691(3)	11.9069(16)
<i>c</i> /Å	12.2135(8)	22.357(3)	16.500(4)	16.924(3)	14.6279(19)
α /deg					102.165(2)
β /deg	106.193(1)	94.057(19)	112.415(5)	113.387(12)	94.135(2)
γ /deg					105.163(2)
<i>V</i> /Å ³	1509.70(18)	2836.8(8)	3298.9(15)	3448.9(11)	1474.5(3)
<i>Z</i>	4	4	8	8	2
cryst size/mm	0.02 × 0.02 × 0.02	0.56 × 0.50 × 0.42	0.32 × 0.32 × 0.10	0.18 × 0.10 × 0.03	0.42 × 0.40 × 0.36
μ /mm ⁻¹	0.307	0.209	0.535	3.075	1.399
no. of data collected	11 829	23 462	18 439	39 649	10 597
no. of unique data	4448	4964	4315	7861	5139
<i>R</i> _{int}	0.023	0.045	0.045	0.065	0.028
data with <i>F</i> ² > 2 σ	3668	3773	3839	5130	4770
no. of refined params	139	248	293	293	260
<i>R</i> (on <i>F</i> , <i>F</i> ² > 2 σ) ^a	0.037	0.056	0.068	0.042	0.049
<i>R</i> _w (on <i>F</i> ² , all data) ^a	0.106	0.172	0.128	0.077	0.089
goodness of fit on <i>F</i> ² ^a	1.038	1.060	1.425	1.046	1.358
min., max. electron density/e Å ⁻³	0.69, -0.37	0.57, -0.47	0.47, -0.30	0.49, -0.47	0.73, -1.89

^a Conventional $R = \sum ||F_o| - |F_c|| / \sum |F_o|$; $R_w = [\sum w(F_o^2 - F_c^2)^2 / \sum w(F_o^2)^2]^{1/2}$; $S = [\sum w(F_o^2 - F_c^2)^2 / (\text{no. data} - \text{no. params})]^{1/2}$ for all data.

Unfortunately, however, the ¹³³Cs nucleus in **11** has a rather short relaxation time, possibly due to fast chemical exchange under the conditions used. In addition, the BH₃ signals in the ¹H spectrum are very broad due to quadrupolar broadening by the ¹¹B nucleus. The combined effect of these two factors is that cross-peaks in the HOESY spectrum corresponding to close proximity between the cesium ion and the BH₃ protons are not distinguishable, and so we are unable to comment on the presence or absence of Cs...H₃B contacts in solution.

Conclusions

Heavier alkali metal complexes of the phosphine-borane-stabilized carbanion (Me₃Si)₂{Me₂P(BH₃)₂}C⁻ are readily accessible via relatively straightforward synthetic procedures. Compounds **6a**, **7**, **10**, and **11** are the first heavier alkali metal complexes of a phosphine-borane-stabilized carbanion to be structurally characterized; the solid state structures of these species vary significantly with increasing ionic radius of the metal. Whereas the sodium complex **6a** crystallizes as a one-dimensional polymer, the isostructural potassium and rubidium complexes **7** and **10** crystallize with a rather complex two-dimensional sheet structure. The corresponding cesium salt has been isolated as an adduct with pmdeta, which crystallizes as a centrosymmetric dimer. For all of these complexes M-BH₃ contacts appear to be an essential feature of their structures; in each case the phosphine-borane-stabilized carbanions bind the metal cations via both their carbanion centers and their BH₃ groups. We expect that such heavier alkali metal complexes will have interesting reactivities that may be complementary to those of their well-established lithium analogues.

Experimental Section

All manipulations were carried out using standard Schlenk techniques under an atmosphere of dry nitrogen. Diethyl ether, THF, toluene, methylcyclohexane, and light petroleum (bp 40–60°C) were distilled under nitrogen from potassium or sodium/potassium alloy; hexamethyldisiloxane was distilled under nitrogen from calcium hydride. THF and hexamethyldisiloxane were stored over

activated 4 Å molecular sieves; all other solvents were stored over a potassium film. Deuterated toluene was distilled from potassium and was deoxygenated by three freeze-pump-thaw cycles and stored over activated 4 Å molecular sieves. The compounds (Me₃-Si)₂{Me₂P(BH₃)₂}CH (**5**),⁶ MeNa,^{8,20} and MeK^{13,21} were prepared by previously published procedures; a single crystal of **5** suitable for X-ray crystallography was obtained from cold (-30 °C) methylcyclohexane containing a few drops of THF. Rubidium and cesium 2-ethylhexoxide were prepared by the direct reaction of 2-ethylhexanol with the elemental metals in light petroleum and were stored as stock solutions in diethyl ether. Butyllithium was obtained from Aldrich as a 2.5 M solution in hexanes and was used as supplied.

¹H, ¹³C{¹H}, ¹¹B{¹H}, and ³¹P{¹H} NMR spectra were recorded on a JEOL Lambda500 spectrometer operating at 500.16, 125.65, 160.35, and 202.35 MHz, respectively. ¹H and ¹³C chemical shifts are quoted in ppm relative to tetramethylsilane; ¹¹B and ³¹P chemical shifts are quoted in ppm relative to BF₃(OEt₂) and 85% H₃PO₄, respectively. Elemental analyses were obtained by the Elemental Analysis Service of London Metropolitan University.

Preparation of [(Me₃Si)₂{Me₂P(BH₃)₂}C]Na(THF)₂(PhMe)_{0.5} (6a**).** A solution of **5** (1.57 g, 6.70 mmol) in cold (-10 °C) diethyl ether (30 mL) was added to solid MeNa (0.27 g, 7.10 mmol). The mixture was allowed to attain room temperature and was stirred for 16 h. The slightly turbid solution was filtered and solvent was removed in vacuo from the filtrate to yield an orange oil. Recrystallization from cold (-30 °C) toluene containing a few drops of THF gave colorless needles of **6a** suitable for X-ray crystallography. Isolated yield: 1.51 g, 87%. Anal. Calcd for C₉H₂₇-BNaPSi₂ (256.26): C 42.18, H 10.62. Found: C 42.11, H 10.69. ¹H{¹¹B} NMR (*d*₈-toluene, 25 °C): δ 0.34 (s, 18H, SiMe₃), 0.58 (d, *J*_{PH} = 15.9 Hz, 3H, BH₃), 1.36 (d, *J*_{PH} = 11.3 Hz, 6H, PMe₂). ¹³C{¹H} NMR (*d*₈-toluene, 25 °C): δ 8.34 (SiMe₃), 22.15 (d, *J*_{PC} = 35.6 Hz, PMe₂) [quaternary carbon not observed]. ¹¹B{¹H} NMR (*d*₈-toluene, 25 °C): δ -28.8 (d, *J*_{PB} = 101.6 Hz). ³¹P{¹H} NMR (*d*₈-toluene, 25 °C): δ -5.6 (q, *J*_{PB} = 101.6 Hz). [Both coordinated THF and toluene of crystallization are rapidly lost under vacuum

(20) Weiss, E.; Corbelin, S.; Cockcroft, J. K.; Fitch, A. N. *Chem. Ber.* **1990**, *123*, 1629.

(21) Weiss, E.; Sauermaun, G. *Angew. Chem., Int. Ed. Engl.* **1968**, *7*, 133; *Chem. Ber.* **1970**, *103*, 265.

and are not observed in either the elemental analysis or the NMR spectra of **6**.]

Preparation of $[(\text{Me}_3\text{Si})_2\{\text{Me}_2\text{P}(\text{BH}_3)\}\text{C}]\text{K}]_\infty$ (7**).** A solution of **5** (2.26 g, 9.65 mmol) in cold (-10°C) diethyl ether (30 mL) was added to solid MeK (0.62 g, 11.45 mmol). The mixture was allowed to attain room temperature and was stirred for 16 h. The solution was filtered and solvent was removed in vacuo from the filtrate to yield a yellow oil. The oil was extracted into hot benzene and filtered. Upon standing at room temperature, colorless blocks of **7** suitable for X-ray crystallography deposited. Isolated yield: 1.48 g, 55%. Anal. Calcd for $\text{C}_9\text{H}_{27}\text{BKPSi}_2$ (272.37): C 39.69, H 9.99. Found: C 39.53, H 10.07. $^1\text{H}\{^{11}\text{B}\}$ NMR (d_8 -toluene, 25°C): δ 0.27 (s, 18H, SiMe_3), 0.40 (d, $J_{\text{PH}} = 14.3$ Hz, 3H, BH_3), 1.32 (d, $J_{\text{PH}} = 9.2$ Hz, 6H, PMe_2). $^{13}\text{C}\{^1\text{H}\}$ NMR (d_8 -toluene, 25°C): δ 8.47 (SiMe_3), 15.16 (Si_2CP), 23.03 (d, $J_{\text{PC}} = 34.6$ Hz, PMe_2). $^{11}\text{B}\{^1\text{H}\}$ NMR (d_8 -toluene, 25°C): δ -27.3 (d, $J_{\text{PB}} = 98.5$ Hz). $^{31}\text{P}\{^1\text{H}\}$ NMR (d_8 -toluene, 25°C): δ -5.9 (q, $J_{\text{PB}} = 98.5$ Hz).

Preparation of $[(\text{Me}_3\text{Si})_2\{\text{Me}_2\text{P}(\text{BH}_3)\}\text{C}]\text{Rb}]_\infty$ (10**).** To a solution of **5** (1.11 g, 4.74 mmol) in diethyl ether (30 mL) was added *n*-BuLi (1.90 mL, 4.74 mmol). This solution was stirred for 2 h, and then a solution of rubidium 2-ethylhexoxide (9.5 mL of a 0.5 M solution in diethyl ether, 4.74 mmol) was added. This mixture was stirred for 2 h and the solvent was removed in vacuo to yield an off-white oil. The oil was dissolved in hot methylcyclohexane, filtered, and allowed to cool to room temperature to give colorless plates of **10** suitable for X-ray crystallography. Isolated yield of crystalline material: 0.49 g, 32%. Anal. Calcd for $\text{C}_9\text{H}_{27}\text{BPRbSi}_2$ (318.74): C 33.91, H 8.54. Found: C 33.91, H 8.40. $^1\text{H}\{^{11}\text{B}\}$ NMR (d_8 -toluene, 25°C): δ 0.23 (s, 18H, SiMe_3), 0.51 (d, $J_{\text{PH}} = 14.4$ Hz, 3H, BH_3), 1.31 (d, $J_{\text{PH}} = 9.2$ Hz, 6H, PMe_2). $^{13}\text{C}\{^1\text{H}\}$ NMR (d_8 -toluene, 25°C): δ 8.45 (SiMe_3), 15.53 (Si_2CP) 23.30 (d, $J_{\text{PC}} = 34.1$ Hz, PMe_2). $^{11}\text{B}\{^1\text{H}\}$ NMR (d_8 -toluene, 25°C): δ -26.7 (d, $J_{\text{PB}} = 97.5$ Hz). $^{31}\text{P}\{^1\text{H}\}$ NMR (d_8 -toluene, 25°C): δ -5.3 (q, $J_{\text{PB}} = 97.5$ Hz).

Preparation of $[(\text{Me}_3\text{Si})_2\{\text{Me}_2\text{P}(\text{BH}_3)\}\text{C}]\text{Cs}(\text{pmdeta})_2$ (11**).** To a solution of **5** (0.89 g, 3.80 mmol) in diethyl ether (20 mL) was added *n*-BuLi (1.52 mL, 3.80 mmol). This mixture was stirred for 2 h, then cesium 2-ethylhexoxide (4.2 mL of a 0.8 M solution in diethyl ether, 3.80 mmol) was added. The resulting solution was stirred for 1 h and then the solvent was removed in vacuo to yield a light brown oil. This oil was washed with hexamethyldisiloxane (3×20 mL), and the residue was dissolved in hot methylcyclohexane (10 mL) and filtered. To the filtrate was added pmdeta (0.79 mL, 3.80 mmol), and the solution was cooled to -30°C for several hours to yield colorless blocks of **11**. Isolated yield: 1.09 g, 53%. Anal. Calcd for $\text{C}_{18}\text{H}_{50}\text{BCsN}_3\text{PSi}_2$ (539.48): C 40.07, H 9.34, N 7.79. Found: C 40.15, H 9.26, N 7.81. $^1\text{H}\{^{11}\text{B}\}$ NMR (d_8 -toluene, 25°C): δ 0.31 (s, 18H, SiMe_3), 0.94 (d, $J_{\text{PH}} = 13.4$ Hz, 3H, BH_3),

1.36 (d, $J_{\text{PH}} = 9.2$ Hz, 6H, PMe_2), 1.95 (s, 3H, NMe), 1.99 (s, 12H, NMe_2), 2.08 (m, 4H, NCH_2), 2.11 (m, 4H NCH_2). $^{13}\text{C}\{^1\text{H}\}$ NMR (d_8 -toluene, 25°C): δ 8.69 (SiMe_3), 16.45 (Si_2CP), 23.99 (d, $J_{\text{PC}} = 34.1$ Hz, PMe_2), 42.75 (NMe), 46.43 (NMe_2), 57.39 (NCH_2), 58.51 (NCH_2). $^{11}\text{B}\{^1\text{H}\}$ NMR (d_8 -toluene, 25°C): δ -25.4 (d, $J_{\text{PB}} = 95.2$ Hz). $^{31}\text{P}\{^1\text{H}\}$ NMR (d_8 -toluene, 25°C): δ -4.4 (q, $J_{\text{PB}} = 95.2$ Hz).

Crystal Structure Determinations of **5, **6a**, **7**, **10**, and **11**.** Measurements for **5** were made at 120 K on a Bruker APEX2 diffractometer using silicon-monochromated synchrotron radiation ($\lambda = 0.6709$ Å); measurements for **6a**, **7**, **10**, and **11** were made at 150 K on Bruker AXS SMART CCD and Nonius Kappa CCD diffractometers using graphite-monochromated Mo $K\alpha$ radiation ($\lambda = 0.71073$ Å). For all compounds cell parameters were refined from the observed positions of all strong reflections in each data set. Intensities were corrected semiempirically for absorption, based on symmetry-equivalent and repeated reflections. The structures were solved by direct methods and were refined on F^2 values for all unique data. Table 2 gives further details. All non-hydrogen atoms were refined anisotropically, H atoms bonded to boron were freely refined isotropically, and the remaining H atoms were constrained with a riding model; $U(\text{H})$ was set at 1.2 (1.5 for methyl groups) times U_{eq} for the parent atom. Disorder was resolved and successfully modeled for one THF ligand in **6a**. Highly disordered toluene solvent in this structure was treated by the SQUEEZE procedure of PLATON.²² Programs were Bruker AXS SMART and APEX2 (control) and SAINT (integration), Nonius COLLECT and associated programs, and SHELXTL for structure solution, refinement, and molecular graphics.²³

Acknowledgment. The authors thank the Royal Society for support, Prof. W. McFarlane for obtaining the ^{133}Cs – ^1H HOESY spectrum of **11**, the EPSRC for funding the UK National Crystallographic Service, and the CCLRC for access to synchrotron facilities.

Supporting Information Available: For **5**, **6a**, **7**, **10**, and **11** details of structure determination, atomic coordinates, bond lengths and angles, and displacement parameters in CIF format. This material is available free of charge via the Internet at <http://pubs.acs.org>. Observed and calculated structure factor details are available from the authors upon request.

OM0606082

(22) Spek, A. L. *J. Appl. Crystallogr.* **2003**, *36*, 7.

(23) (a) SMART, APEX2, and SAINT software for CCD diffractometers; Bruker AXS Inc.: Madison, WI, 2004 and 1997. (b) Sheldrick, G. M. *SHELXTL user manual*, version 6; Bruker AXS Inc.: Madison, WI, 2001. (c) COLLECT software; Nonius BV: Delft, The Netherlands, 2000.